SYNTHESIS AND CHARACTERIZATION OF L-ASPARAGINASE ENCAPSULATED POLY-L-LYSINE-GRAFT-POLY(ETHYLENE) GLYCOL POLYMER NANOPARTICLES FOR POTENTIAL THERAPEUTIC DELIVERY APPLICATIONS

A thesis presented to the faculty of the Graduate School of Western Carolina University in partial fulfillment of the requirements for the degree of Master of Science in Chemistry

By

Keri Joanna Goff

Director: Dr. Rangika Hikkaduwa Koralege

Assistant Professor of Chemistry

Department of Chemistry and Physics

Committee Members: Dr. Maria Gainey, Chemistry

Dr. Channa De Silva, Chemistry

28th March 2022

ACKNOWLEDGMENTS

I would like to thank the various assistantships, who have funded my expenses throughout this research project: the WCU Summer 2021 Research Assistantship and the many semesters of Teaching Assistantships.

I would like to express my deepest appreciation to my research advisor, and mentor, Dr. Rangika Hikkaduwa Koralege, for her exceptional assistance and guidance throughout this entire project, and for making it a success. She has expanded my knowledge on topics my past self could not have begun to comprehend. I have learned so much from her, and I know she will always be someone I can come to for counsel.

I am also extremely grateful to my committee members, Dr. Maria Gainey and Dr. Channa De Silva, for all of their guidance and assistance with this project. Their constructive criticism challenged me to grow, and I wouldn't be where I am now without that push. I am also grateful to Dr. Al Fischer for taking the time to teach me how to use multiple instruments and guiding me through the process whenever I was confused. Thank you to Mr. Wes Bintz for all of the chemicals and supplies from the stockroom. I would also like to acknowledge all of the professors of the graduate classes that I took.

I cannot begin to express my thanks to my family and friends that have supported me throughout this project. They have kept me rooted throughout the years, especially when I felt in over my head. My family and friends have helped mold me into the person I am today.

Lastly, I would like to thank the rest of the WCU Department of Chemistry and Physics. I have met some of the kindest people during my time at WCU. I will never forget the impact you have all made on my life.

TABLE OF CONTENTS

LIST OF TABLES

LIST OF FIGURES

LIST OF ABBREVIATIONS AND SYMBOLS

L-ASNase—L-asparaginase

PLL—poly-L-lysine

PEG—poly-ethylene glycol

PLL-g-PEG—Poly-L-lysine-graft-poly(ethylene) glycol

NPs—nanoparticles

RBCs—red blood cells

PBS—phosphate buffered saline

PEG-ASNase—pegylated-L-ASNase

°C - degree Celsius

μL – microliter

PDI – Polydispersity index

nm – nanometer

d.nm – diameter in nanometers

CS—chitosan

IVH—intraventricular hemorrhage

RGD—arginine-glycine-aspartic acid

uPA—urokinase-type plasminogen activator

ABSTRACT

SYNTHESIS AND CHARACTERIZATION OF L-ASPARAGINASE ENCAPSULATED POLY-L-LYSINE-GRAFT-POLY(ETHYLENE) GLYCOL POLYMER NANOPARTICLES FOR POTENTIAL THERAPEUTIC DELIVERY APPLICATIONS

Keri Joanna Goff

Western Carolina University, 28th March 2022

Director: Dr. Rangika Hikkaduwa Koralege

L-asparaginase (L-ASNase) is a therapeutic enzyme that is widely used for the treatment of hematopoietic diseases such as acute lymphoblastic leukemia and lymphomas since 1970. L-ASNase can destroy asparagine dependent tumors by degrading circulating L-asparagine and destroying malignant cells. Being a therapeutic enzyme and essentially a protein drug, L-ASNase has intrinsic drawbacks such as low stability, short circulating lifetime, and low catalytic activity under physiological conditions. Due to the bacterial origin of L-ASNase, immunogenicity is another major problem with high frequency of hypersensitivity reactions. L-ASNase delivered via pegylated-L-ASNase (PEG (poly(ethylene)glycol)-ASNase) form has been shown to improve clinical outcome of this therapy. The focus of this project is to successfully encapsulate a catalytically active, stable, therapeutic protein in PLL-g-PEG NPs.

The goals of this project include (1) synthesis and characterization a PLL-g-PEG co-polymer, (2) synthesis of protein-polymer nanoparticles by encapsulating a model protein, bovine serum albumin (BSA) in PLL-g-PEG , (3) synthesis of protein-polymer nanoparticles by encapsulating therapeutic protein L-ASNase in PLL-g-PEG , (4) perform physicochemical characterization including nanoparticle size and surface charge, (5) evaluate encapsulation efficiency of L-

ASNase in NPs, (6) evaluate stability of NPs under physiological conditions, and (7) evaluate enzymatic activity of encapsulated L-ASNase.

In the present study, we have successfully synthesized and characterized a maleimide functionalized PLL-g-PEG co-polymer. Nanoparticles were formed through electrostatic interactions of the cationic backbone of the PLL-g-PEG copolymer and negatively charged L-ASNase. L-ASNase nanoparticles had an average hydrodynamic diameter of 114.5 ± 5.66 nm and a near neutral zeta potential of 0.436 ± 0.258 mV. The extent of L-ASNase encapsulation was determined to be 100% according to the SDS-PAGE data. Additionally, SDS-PAGE data provides conclusive results that these therapeutic nanoparticles are stable in solution at physiological pH conditions for more than 6 months and long-term particle stability studies are in progress. Encapsulated L-ASNase showed an average of 10.5 nmole/min/mL activity and that is 53% as a percentage compared to the free L-ASNase positive control. These particles were stable in 10% FBS for more than 17 hours at 37 °C. In conclusion, we were able to successfully encapsulate a catalytically active, stable, therapeutic protein in PLL-g-PEG NPs.

CHAPTER ONE: INTRODUCTION

1.1 Nanomaterials in drug delivery

Nanomaterials have gained a lot of interest due to their tunable physical, chemical, and biological properties with enhanced performance over their bulk counterparts. Nanomaterials are described as materials with length of 1–1000 nm in at least one dimension. However, most commonly used nanomaterials have diameters in the range of 1 to 100 nm.[1] Nanotechnology and the use of nanomaterials has caused rapid development in the process of diagnosis and treatment of diseases.

Various types of nanomaterials have been used as drug carriers, including targeted delivery methods. These delivery methods can be triggered by environmental, pH, thermal responses, and enhanced biocompatibility.[2] Nanomaterials in drug delivery have been found to improve the cellular uptake of poorly soluble drugs as well as enhance drug bioavailability at effective doses. Studies have shown drugs wrapped by nanomaterials prolong their circulation time. This can improve the biodistribution and pharmacodynamics of the therapeutics. Nanomaterials modified by other bioactive molecules can exhibit distinct functions, such as specific targeting or the characteristics of environmental responsiveness, thereby facilitating in drug accumulation and better reaching its effective dose.[2] Commonly used nanomaterials in drug delivery include biopolymeric materials and lipid systems.[3]

A commonly used biopolymeric material is chitosan (CS).[2] CS is a natural polysaccharide that is mainly obtained from marine crustaceans. CS is one of the most abundant biopolymers derived from natural chitin. CS is a polysaccharide that contains positively charged amine groups. The polysaccharide is found to be promising for drug delivery due to its biocompatibility, biodegradability, low toxicity, and structural variability. Due to its low

solubility and poor mechanical properties, CS has not been extensively utilized in the clinic and requires further research and modifications. A wide range of CS derivatives have been found to have improved solubility and the ability to self-assemble. These derivatives have been applied in various biomedical and pharmaceutical processes. CS-based nanomaterials could potentially optimize the transport of drugs. This could lead to the improvement of drug efficacy and targeted drug therapy.[2]

Lipid systems such as liposomes and micelles were the very first generation of nanoparticle-based therapy.[3] These lipid systems can contain inorganic nanoparticles like gold or zinc. These properties led to an increase in the use of inorganic nanoparticles in drug delivery, imaging, and therapeutic functions. Liposomes were discovered in the 1960s and have been used in the pharmaceutical and cosmetics industry for the transportation of diverse molecules. Liposomes are one of the most studied carrier systems for drug delivery. They are vesicles of spherical form composed of phospholipids. The membrane of liposomes is analogous to the cell membranes and are able to facilitate the incorporation of drugs. There are four types of liposomes: (1) conventional type liposomes, (2) PEGylated type, (3) ligand-targeted type, and (4) theragnostic type liposomes. There are drawbacks to using liposomes as a carrier system such as reticuloendothelial system, opsonization, and immunogenicity. However, liposomes have been proven to make therapeutic compounds stable, improve biodistribution, can be used with hydrophilic and hydrophobic drugs, and are biocompatible and biodegradable.[3]

1.2 Protein-polymer nanoparticles

Therapeutic proteins have shown to be an effective treatment against a variety of diseases. Unlike traditional small-molecule chemotherapeutics, protein therapeutics can be actively targeted towards malignant cells using cell surface receptors and/or other markers

specifically associated with or overexpressed on tumors versus healthy tissue.[4] Protein therapeutics can mainly be grouped into four categories: (1) proteins with enzymatic or regulatory activity, (2) proteins that block, stimulate, or tag their molecular targets, (3) vaccines, and (4) diagnostics. Proteins therapeutics with enzymatic activity are used for the treatment of various diseases. These enzymes often bind and act on their targets with great affinity and specificity. They are also catalytic and convert multiple target molecules to the desired products. These features make therapeutic enzymes specific and potent drugs for many disorders.[4-6] Enzyme diagnostics use enzymes to diagnose and analyze biological abnormalities. Although therapeutic proteins have been used widely in drug discovery and development, there are certain challenges that still need to be addressed. Some of the protein-based therapeutics have been reported to induce immune responses and some other unwanted reactions.

Urokinase is an example of a commonly used therapeutic enzyme and it helps the body produce a substance that dissolves unwanted blood clots. The enzyme is made in the kidney and found in the urine. Urokinase is commonly used to treat blood clots in lungs. One study focused on intraventricular hemorrhage (IVH). IVH is bleeding inside or around the ventricles in the brain and intraventricular urokinase has been used to treat IVH patients. It has been found that intraventricular urokinase may significantly improve 30-day survival in IVH patients.[7] Some studies have shown that arginine-glycine-aspartic acid (RGD) modified pH-triggered delivery system for the urokinase-type plasminogen activator (uPA) is resistant to enzyme degradation. It has been reported that uPA-loaded nanogels could significantly prolong the lifetime of uPA.[8]

Polysaccharides and proteins are collectively called natural biopolymers and are extracted from biological sources such as animals, plants, microorganisms, and marine sources.[3] Protein-based nanoparticles are generally decomposable, metabolizable, and are easy to functionalize for

its attachment to specific drugs and other targeting ligands. Protein-based nanoparticles are generally produced using one of two systems: (1) from water-soluble proteins like bovine and human serum albumin or (2) from insoluble ones like zein and gliadin. These nanoparticles can be altered to combine targeting ligands that identify exact cells and tissues to promote their targeting mechanism. One of the main drawbacks of polysaccharides is its degradation characteristics at high temperatures. Techniques such as crosslinking of the polymer chains have been employed to stabilize the polysaccharide chains. These biopolymers are successful in drug delivery due to their versatility and specified properties. Protein-based nanoparticles are excellent candidates for further development as drug delivery systems.[3]

Poly-L-lysine (PLL) and poly-ethylene glycol (PEG) are commonly used polymers for drug delivery. PLL polymers can be used in promoting cell adhesion to solid substrates, conjugation to methotrexate for increased drug transport, microencapsulation of islets, cell microencapsulation technology, and chromosomal preparations.[9] PLL has the ability to self-assemble with negatively charged proteins, such as L-asparaginase. The bioavailability is markedly improved over free enzyme. PEG is widely utilized in drug delivery and nanotechnology due to its reported "stealth" properties and biocompatibility. Studies have shown that PEGylation allows particulate delivery systems and biomaterials to evade the immune system. This ability prolongs circulation lifetimes.[10] PEG reduces clearance and provides a convenient terminal for ligand attachment. PEG 5 kDa has a maleimide group attached for peptide attachment. These peptides will be used to target and infiltrate RBCs.

1.3 L-asparaginase in therapeutic applications

L-asparaginase (L-ASNase) is a therapeutic enzyme commonly used for the treatment of hematopoietic diseases such as acute lymphoblastic leukemia (ALL) and lymphomas. It has been

used for these treatments since the 1970s. This therapeutic enzyme is a tetramer with four identical subunits. Figure 1 shows the crystal structure of the protein.[11] Each color represents one of the four identical subunits. The molecular weight of L-ASNase is 136.32 kDa.

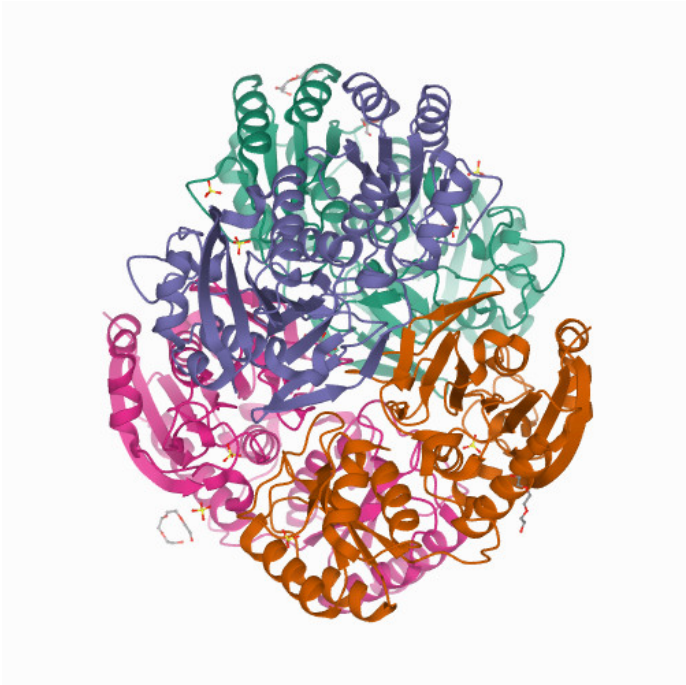

Figure 1: Crystal Structure of L-ASNase.[11] (PDB DOI: 10.2210/pdb1O7J/pdb)

ALL is a type of cancer of the blood and bone marrow. This disease occurs when a bone marrow cell develops mutations in its genetic material or DNA. The disease progresses rapidly and creates immature blood cells. ALL mainly affects lymphocytes, which are white blood cells. L-ASNase is able to destroy asparagine dependent tumors by degrading circulating L-asparagine in the blood. Lymphoblasts cannot produce L-asparagine independently, so they obtain it from the blood. L-ASNase works by depriving the lymphoblasts of their L-asparagine source. This leads to the destruction of the malignant cells. This process is shown in Figure 2.

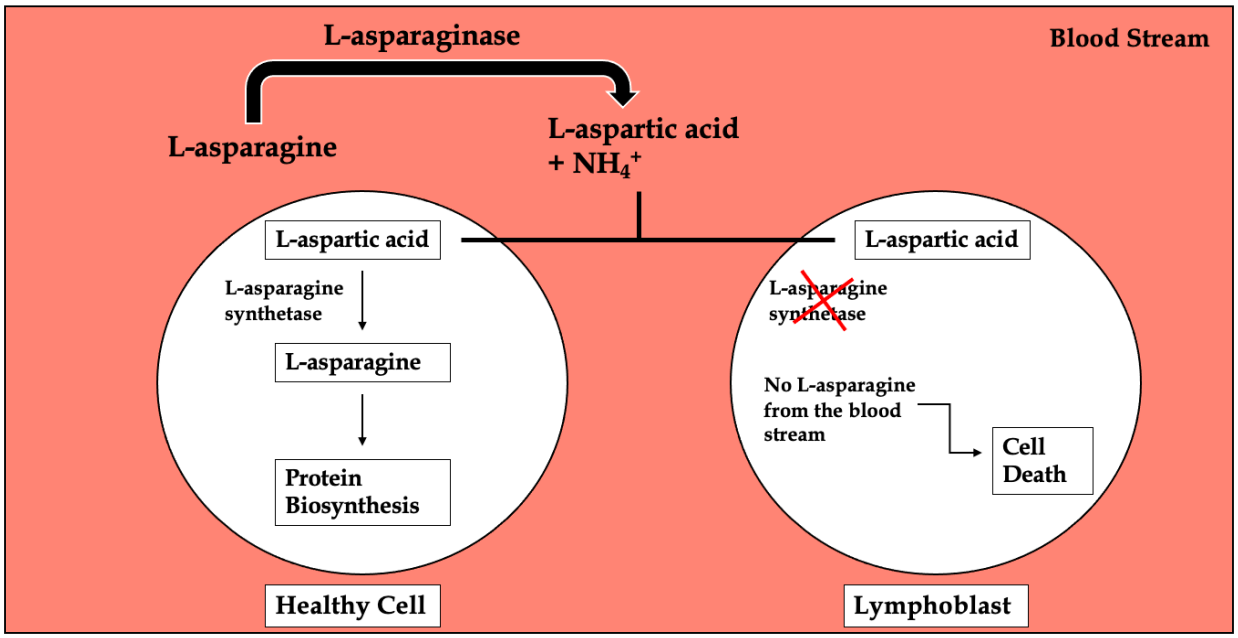

Figure 2: How L-ASNase destroys L-asparagine dependent tumors.

However, L-ASNase has intrinsic drawbacks such as low stability, short circulating lifetime in the blood stream, and low catalytic activity under physiological conditions.[12-14] Research has suggested that the encapsulation of L-ASNase increases the efficiency and stability of the enzyme and provides efficient protection against enzymatic degradation. Studies have been done to compare native L-ASNase and pegylated L-ASNase. Patients treated with native L-ASNase had high-titer antibodies. This is associated with low L-ASNase activity in the native arm. L-ASNase delivered by pegylated-L-ASNase (PEG-ASNase) form has been shown to improve clinical outcome of this therapy. The patients treated with PEG-ASNase had more rapid clearance of lymphoblasts as well as more prolonged L-ASNase activity than those treated with native L-ASNase.[15]

To address the drawbacks of L-ASNase, our primary goal of this project is to synthesize and characterize L-asparaginase encapsulated PLL-g-PEG polymer nanoparticles. The successful encapsulation of catalytically active L-ASNase in nanoparticles is important for its therapeutic

activity. Our long-term goal is to develop a nanoparticle system that is capable of entering red blood cells (RBCs) to extend therapeutic circulation time and therapeutic loading capacity for improved treatment of blood-specific diseases. Additionally, this project could potentially lead to a more efficient method of drug delivery using red blood cells.

1.4—Research Goals and Expected Outcomes

The goals of this project are to (1) synthesize and characterize a PLL-g-PEG co-polymer, (2) synthesize protein-polymer nanoparticles by encapsulating a model protein, bovine serum albumin (BSA) in PLL-g-PEG , (3) synthesize protein-polymer nanoparticles by encapsulating therapeutic protein L-ASNase in PLL-g-PEG , (4) perform physicochemical characterization including nanoparticle size and surface charge, (5) evaluate encapsulation efficiency of L-ASNase in NPs, (6) evaluate stability of NPs under physiological conditions, and (7) evaluate enzymatic activity of encapsulated L-ASNase.

In this project we are planning to address the following key questions. (1) can we successfully encapsulate the therapeutic enzyme in a polymeric NP construct? (2) what is the average hydrodynamic size and surface charge of theses NPs? (3) are the NPs stable under physiological pH conditions and for how long? (4) is the enzyme catalytically active within the NP construct? (5) can the enzyme leach out of NPs with time?

The successful encapsulation of catalytically active L-ASNase in a stable polymeric nanoparticle construct will be significant in the field of drug delivery to blood specific diseases such as ALL and research outcomes of this project will have broad applicability in the field of drug delivery and cancer therapy.

CHAPTER TWO: EXPERIMENTAL METHODS

2.1—Materials

Poly-L-lysine•HBr with a molecular weight of 15-30 kDa, fluorescein isothiocyanate labelled bovine serum albumin (FITC-BSA), fetal bovine serum, L-asparaginase, and asparaginase activity assay kit were purchased from Sigma-Aldrich. Heterobifunctional PEG MAL (Maleimide-PEG-NHS) and mPEG-NHS with molecular weights of 5 and 2 kDa, respectively, were purchased from Creative PEGWorks. Bovine serum albumin, Glutaraldehyde (50%), acrylamide/bisacrylamide (37.5:1) and other polyacrylamide gel casting and running materials were purchased from Fisher Scientific. The reagents were used without further purification. Ultrapure water with a resistivity of 18.2MΩ was obtained from a Barnstead EASYpure II RF/UV Ultrapure Water System.

2.2—PLL-g-PEG Co-polymer Synthesis

Primary amine groups of the PLL backbone were modified with the succinimidyl ester group on the heterobifunctional PEG to produce PLL-g-PEG. To prepare PLL-g-PEG, 15 mg of 15-30 kDa PLL•HBr was dissolved in 200 μL of phosphate buffered saline (PBS, pH 7.4) and a 50/50 mass ratio mixture of 2 kDa mPEG-NHS (20 mg) and 5 kDa MAL-PEG-NHS (20 mg) solids were added to the dissolved PLL. The mixture was allowed to react for 1 h before being washed three times with 50/50 (v/v) mixture of PBS and ethanol, and a final wash with pure ethanol in a 10 kDa centrifugal concentrator. After the washes, the copolymer was air dried manually using an air valve before being used or stored at -20°C. This procedure is depicted in Figure 3.

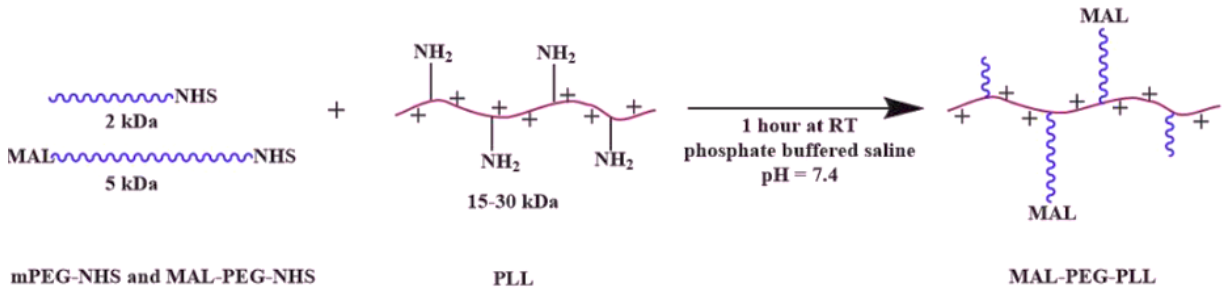

Figure 3: Synthesis of PLL-g-PEG Co-polymer.

2.2.1—Modifications in PLL-g-PEG Co-polymer Drying Procedure

The original method required the copolymer to be air dried manually using an air valve before being used or stored at -20°C. The modified drying method used a rotary evaporator operating at 280-350 rpm without heat. This method was slightly longer than the manual method, but the copolymer was more accessible for future use and there was less chance for the solution to splash out of the scintillation vial.

2.3—Synthesis of Bovine Serum Albumin (BSA) Encapsulated Nanoparticles

A BSA stock solution of 1 mg/mL was prepared by taking 1 mg of BSA and dissolving in 1 mL of PBS. Samples of BSA were encapsulated using PLL-g-PEG (15-30 kDa), with a copolymer:protein mass ratio of 7:1. BSA was dissolved in PBS to a concentration of 0.266 mg/mL and maleimide functionalized PLL-g-PEG copolymer was dissolved in PBS at a concentration of 6 mg/mL. The copolymer (7.5 uL) was then added to the BSA solution (25 uL) dropwise, while gently vortexing, followed by incubation of the mixture of 1 hour at room temperature. To stabilize the polyion complexes formed in this study, amino groups within the particles were cross-linked with 5 uL of glutaraldehyde solution (0.025% in PBS) and incubated for another 3 hours at room temperature.[16-18]

2.4—Synthesis of L-asparaginase (L-ASNase) Encapsulated Nanoparticles

A L-ASNase stock solution of 1 mg/mL was prepared by taking 1 mg of L-ASNase and dissolving in 1 mL of PBS. Samples of L-ASNase were encapsulated using PLL-g-PEG (15-30 kDa), with a copolymer:protein mass ratio of 7:1. L-ASNase was dissolved in PBS to a concentration of 0.266 mg/mL and maleimide functionalized PLL-g-PEG copolymer was dissolved in PBS at a concentration of 6 mg/mL. The copolymer (7.5 uL) was then added to the L-ASNase solution (25 uL) dropwise, while gently vortexing, followed by incubation of the mixture of 1 hour at room temperature. To stabilize the polyion complexes formed in this study, amino groups within the particles were cross-linked with 5 uL of glutaraldehyde solution (0.025% in PBS) and incubated for another 3 hours at room temperature.[16-18] This procedure is depicted in Figure 4.

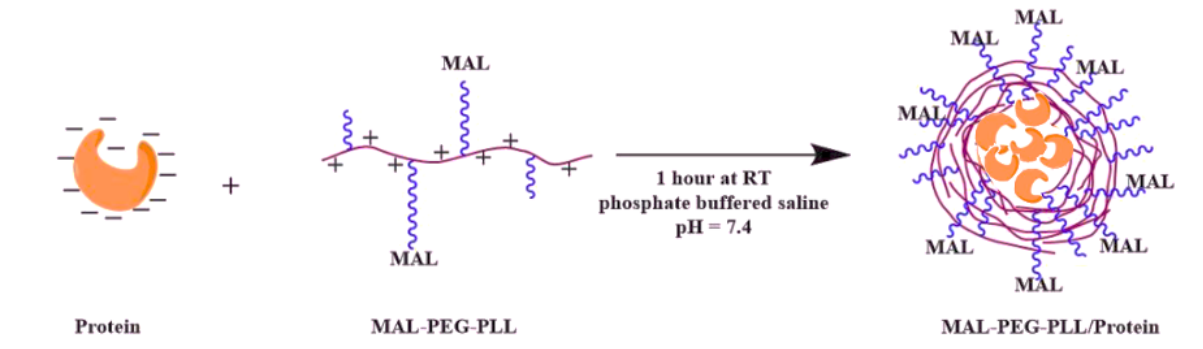

Figure 4: Synthesis of L-ASNase encapsulated NP Synthesis.

2.4.1—Modifications in L-ASNase Encapsulated Nanoparticle Procedure

To obtain monodispersed nanoparticles that are less than 100 nm, vortexing steps in the L-asparaginase nanoparticle synthesis procedure were modified as summarized in Table 1.

Table 1: Modified Procedures for L-ASNase Nanoparticle Synthesis

	Vortex	Shaker (1-hour)	Shaker (3-hours)
Procedure 1 (Standard)	✓	-	-
Procedure 2	✓	-	✓
Procedure 3	-	✓	✓ (briefly)

2.4.2—Optimized L-ASNase Encapsulated Nanoparticle Synthesis Procedure

The optimized L-ASNase encapsulation procedure followed the original method with some modifications in the polymer addition step. Addition of the polymer solution was done by inserting the pipette tip into the protein solution followed by vortexing and simultaneous release of the polymer. This procedure was followed when adding PLL-g-PEG to the L-ASNase solution and adding glutaraldehyde to the polymer/protein mixture.

2.5—^{1}HNMR Analysis

PLL-g-PEG polymer (5 mg), PLL (5 mg), PEG 2 kDa (5 mg), and PEG 5 kDa (5 mg) were dissolved in d-DMSO (0.5 ml) and analyzed using JEOL 300 MHz Eclipse NMR with a 5-mm tunable probe for ^{1}H NMR. Using d-DMSO led to a large water peak in the middle of the target peaks, causing large amounts of noise.

To avoid noise, PLL-g-PEG polymer (5 mg), PLL (5 mg), PEG 2 kDa (5 mg), and PEG 5 kDa (5 mg) were dissolved in d-$CDCl_3$ and analyzed using Bruker 400 MHz NMR with a 5-mm tunable probe for ^{1}H NMR. This method was highly successful with the exception of PLL. PLL was found to not be soluble in d-$CDCl_3$.

2.6—Physicochemical Characterization of Nanoparticles

The size distribution of L-ASNase NPs (100 uL) was determined using DLS on a Malvern Zetasizer ZS Particle Size Analyzer equipped with a 4 mW 632.8 nm laser. All the

measurements were done at 25 °C and using a Brand Tech Scientific ZEN0040 70 μL Ultra-Micro disposable cuvette, with stopper. Some NP samples were filtered using 0.45 μm filters before DLS. The ζ-potential was determined by using phase analysis light scattering (PALS) using a DTS1070 cell. ζ-potentials were calculated from the electrophoretic mobility measurements using Smoluchowski's equation.[19]

2.7—Gel Retardation Assay

The extent of L-asparaginase encapsulation into NPs was determined by a gel retardation assay. SDS-PAGE gels (8% and 12%) were hand casted and loaded with either NP samples or a control of non-encapsulated L-asparaginase protein. NPs were run at 180 V under non-reducing conditions using a BIO RAD Mini-PROTEAN® Tetra Cell apparatus until the dye front reached the bottom of the gel. The SDS-PAGE gels were stained with Coomassie G-250 before imaging. SDS-PAGE gels were run on 0-, 3-, 8-, 10-, 15-, 17-, 53-, 56-days, 3- months and 6-months old NPs.

Hand casted Native PAGE gels (12%) were also run at 180 V using a BIO RAD Mini-PROTEAN® Tetra Cell apparatus until the dye front reached the bottom of the gel. The Native PAGE gels were stained with Coomassie G-250 before imaging.

2.7.1—Boiling of L-ASNase

To denature proteins before loading, the samples were incubated at 95 degrees for 5 minutes in our loading buffer, Laemmli SDS Sample Buffer (non-reducing), plus 2-Mercaptoethanol. The loading buffer contained dye, beta mercaptoethanol (BME), glycerol, and SDS.

2.8—Asparaginase Activity Assay

This assay was used to evaluate the activity of L-ASNase in NPs. Asparaginase activity assay kit (Catalog Number: MAK007) was purchased from Sigma-Aldrich. Asparaginase activity was calculated by measuring the amount of aspartate generated in a coupled enzymatic reaction using colorimetric detection. A series of aspartate standard solutions were used as calibration standards. The samples were analyzed using the SpectraMax iD5 multimode plate reader at a wavelength of 570 nm.

2.8.1—Preparation of Aspartate Standards for Colorimetric Detection

A 10 μL aliquot of aspartate standard solution with a concentration of 100 mM was added into 990 μL of asparaginase assay buffer to prepare a 1 mM standard solution. Volumes of 0, 2, 4, 6, 8, and 10 μL of the 1 mM aspartate standard solution was added into a 96 well plate to generate 0 (blank), 2, 4, 6, 8, and 10 nmoles/well standards. An aliquot of asparaginase assay buffer was added to each well to bring the total volume of each well to 50 μL.

2.8.2—Preparation of L-ASNase NPs for Colorimetric Detection

L-ASNase NP samples with volumes of 50, 25, 10, and 5 μL were used for the assay reaction. The final volume of each sample was made to 50 μL using the asparaginase assay buffer as similar to the standard solutions prepared in section 2.8.1. For the positive control, 5 μL of asparaginase assay positive control was used and the final volume was adjusted to 50 μL with water.

2.8.3—Assay Reaction

Table 2: Reaction Mixes

Reagent	Samples and Standards	Sample Blank
Asparaginase Assay Buffer	40 uL	42 uL
Substrate Mix	4 uL	4 uL
Aspartate Enzyme Mix	2 uL	-
Conversion Mix	2 uL	2 uL
Fluorescent Peroxidase Substrate	2 uL	2 uL

2.9—Measuring Nanoparticle Stability

NP stability (FITC-BSA release) at physiological conditions was assessed by measuring potential release of encapsulated FITC-BSA from the NPs at 37 °C as a function of time. For this study, samples (5 μg equivalent FITC-BSA encapsulated NP or non-encapsulated FITC-BSA as a control) were diluted in 3 mL of 10% FBS and placed in a well plate with a lid cover and magnetic stirrer. FITC-BSA release from the NPs was measured every 5 minutes and then every day using excitation wavelength of 488 nm and fluorescence emission at 530 nm wavelength.

CHAPTER 3: RESULTS AND DISCUSSION

3.1—Characterization of PLL-g-PEG co-polymer using ^{1}H NMR

PLL-g-PEG co-polymer was synthesized using 2 and 5 kDa PEG and PLL. PLL, PEG (2 kDa), PEG (5 kDa), and PLL-g-PEG co-polymer was characterized using ^{1}H NMR spectroscopy. Figure 7 shows the ^{1}H NMR spectrum of PLL in *d*-DMSO.

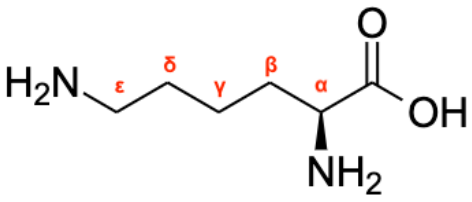

Figure 5: Poly-L-lysine structure.

β, γ, and δ -CH_2 peaks of PLL are shown at 1-2 ppm. Figure 8 shows the ^{1}H NMR spectrum of PLL-g-PEG copolymer in *d*-DMSO, and Table 3 summarizes the chemical shifts observed for each functional group. PEG functional groups shown at 3.7 ppm and 3.3-3.4 ppm confirms that PEG was successfully grafted onto PLL.

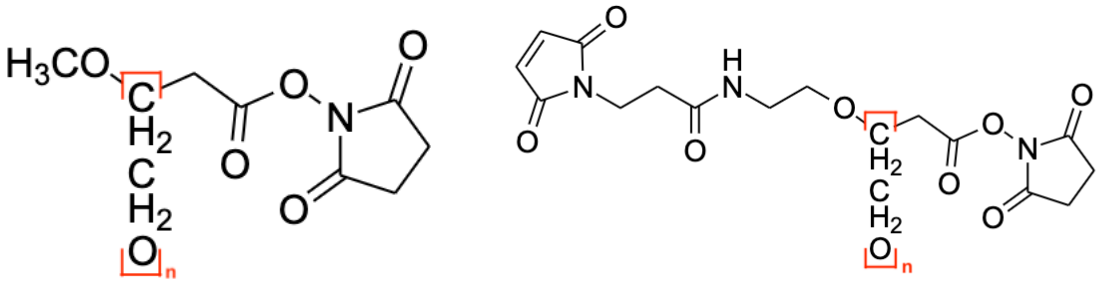

Figure 6: Poly-ethylene glycol 2 kDa (left) and MAL-PEG 5 kDa (right) structures.

The *d*-DMSO solvent peak at approximately 3.3 ppm was causing a large amount of noise to our target chemical shifts. A better signal to noise ratio in NMR spectra was achieved by

using deuterated chloroform ($CDCl_3$) solvent. Figures 9-11 show the ^1H NMR spectra of PEG (2 kDa), PEG (5 kDa), and PLL-g-PEG in $CDCl_3$ respectively. By using $CDCl_3$ the prominent water peak shown at 3.3 ppm in DMSO spectra was eliminated. This allowed for spectra with much less baseline noise compared to *d*-DMSO. However, PLL was not soluble in $CDCl_3$.

Table 3: Chemical Shifts for PLL-g-PEG in *d*-DMSO

Functional Group	Chemical Shift
β,γ, and δ -CH_2 peaks of lysine	1-2 ppm
-CH_2CH_2O- of PEG	3.7 ppm
-OCH_3 of PEG	3.3-3.4 ppm
-CH- of PLL	4.1-4.3 ppm

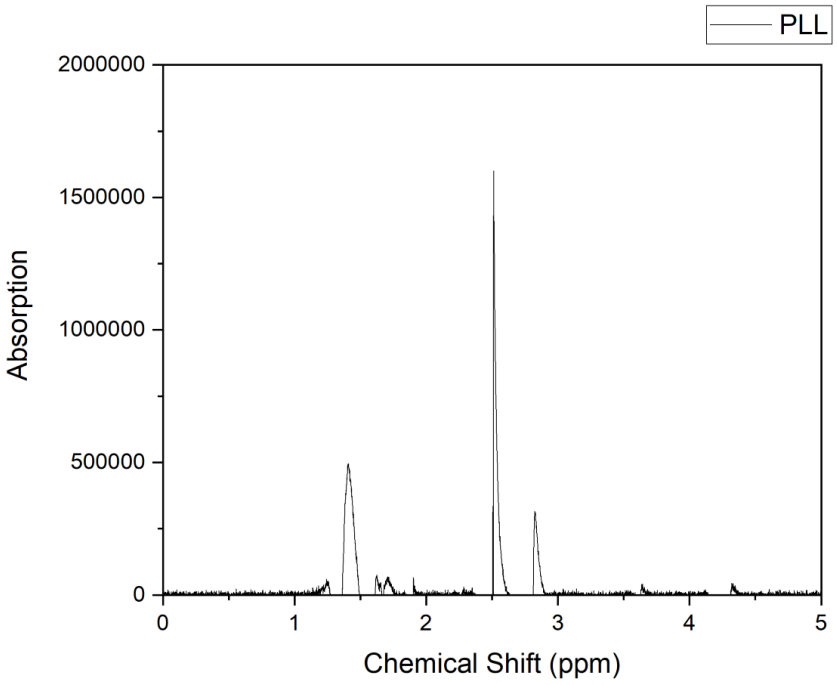

Figure 7: ^1H NMR spectrum of HBr•PLL in *d*-DMSO.

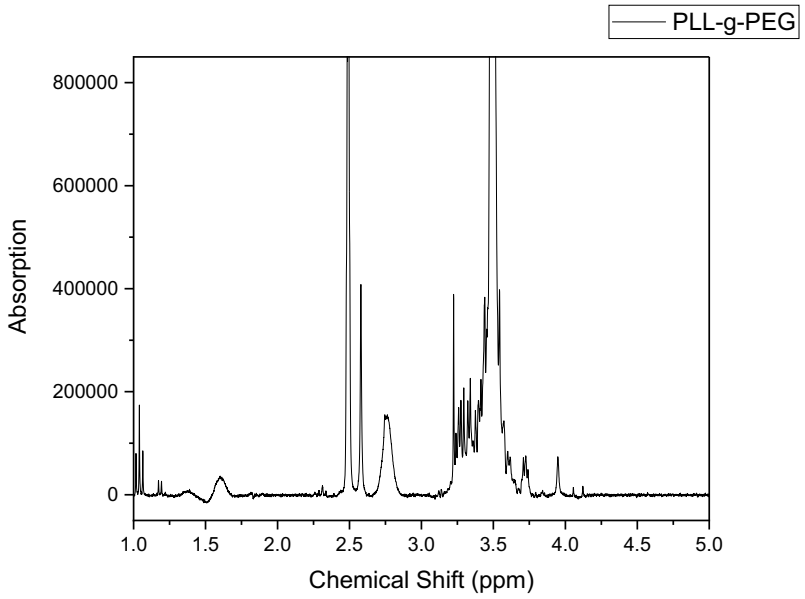

Figure 8: ^{1}H NMR spectrum of PLL-g-PEG co-polymer in *d*-DMSO.

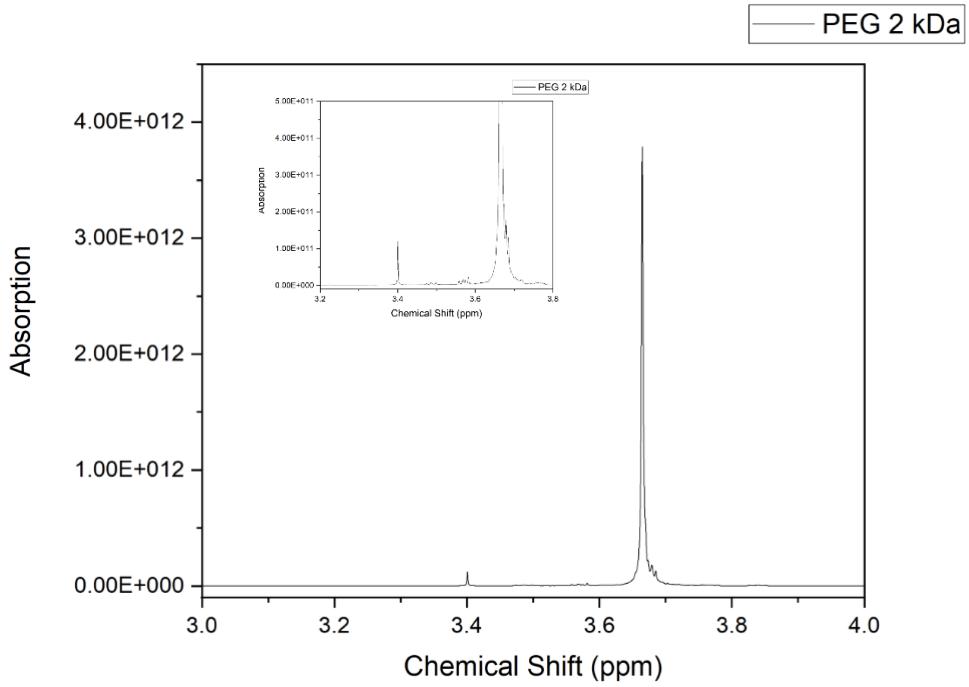

Figure 9: ^{1}H NMR spectrum of PEG (2 kDa) in $CDCl_3$

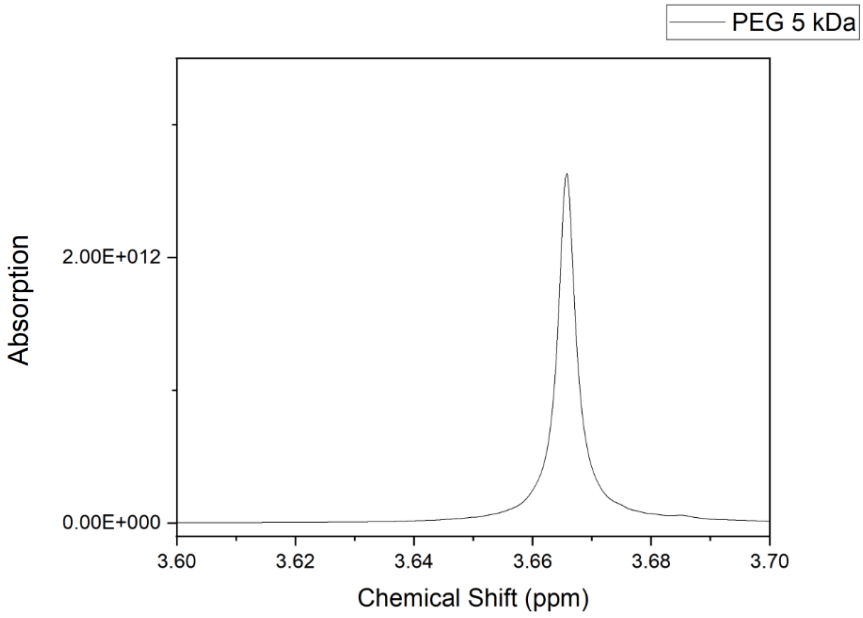

Figure 10: ^{1}H NMR spectrum of PEG (5 kDa) in $CDCl_3$

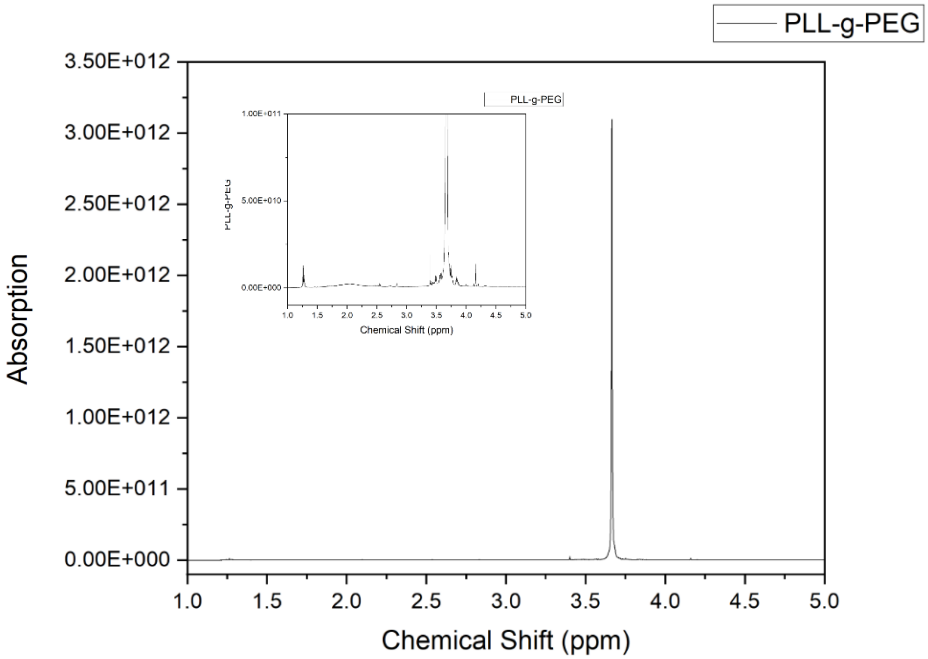

Figure 11: ^{1}H NMR spectrum of PLL-g-PEG copolymer in $CDCl_3$

3.2—Physicochemical Characterization of BSA and L-ASNase Nanoparticles

NP size and ζ-potential data obtained using DLS and PALS respectively, are given as the mean and standard deviation of three replicates (Figures 12-17). DLS is a technique that primarily measures the Brownian motion of macromolecules in solution that arises due to bombardment from solvent molecules and relates this motion to the size of the nanoparticles. Zeta potential is the potential difference between the dispersion medium and the stationary layer of fluid attached to the particle. This method is used to find the surface charge of a particle.[20]

BSA encapsulated NPs have been synthesized as a model protein NP construct to evaluate the particle characteristics. Figure 12 shows particle size distribution of BSA NPs. BSA NPs had an average hydrodynamic diameter of 17.83 ± 1.4 nm and an average polydispersity index (PDI) of 0.302 ± 0.022. The PDI is an important parameter that describes the width or spread of the particle size distribution. PDI values can vary from 0 to 1, where the particles with PDIs less than 0.1 implies monodispersed particles and the values more than 0.1 may imply polydispersed particle size distributions. Even though the average hydrodynamic diameter was 17.83 nm, the BSA NP sample was polydisperse according to the PDI. The zeta potential of BSA nanoparticles was found to be -0.66 ± 0.09 mV. The electrostatic attractions between the positively charged polymer backbone and the negatively charged BSA protein results in near neutral surface charge in NPs. However, the net negative surface charge of the NPs may suggest the presence of protein near the particle surface.

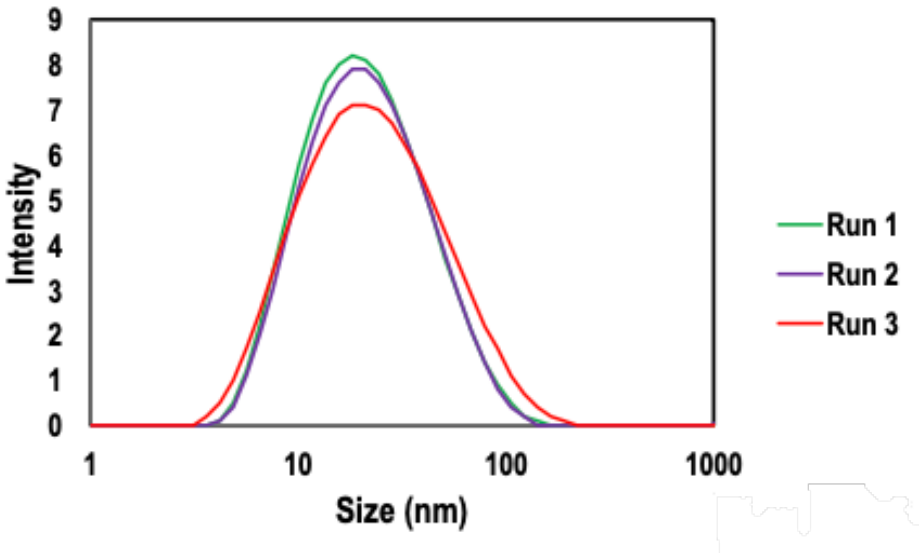

Figure 12: Particle size distribution of BSA nanoparticles.

Encapsulation of the therapeutic protein L-ASNase in PLL-g-PEG was carried out using different concentrations of protein and different vortexing/shaking conditions as described in Table 1 to achieve a narrow size distribution and a better encapsulation. To evaluate the effect of protein concentration on encapsulation, two different protein concentrations were used. Figure 13 (a) and (b) shows DLS data for L-asparaginase NPs prepared at an initial protein concentration of 0.133 mg/ml and 0.266 mg/ml respectively. As evident from the graphs those NPs were polydisperse. A filtering step was introduced in the procedure to achieve narrow distributions. Filtering with 0.45 μm filters did not improve the monodispersity as shown in Figure 8 (a) and (b). The PDI of these samples were approximately 0.500 to 1.000. In conclusion, varying the protein concentration and filtration before DLS did not improve monodispersity of these samples.

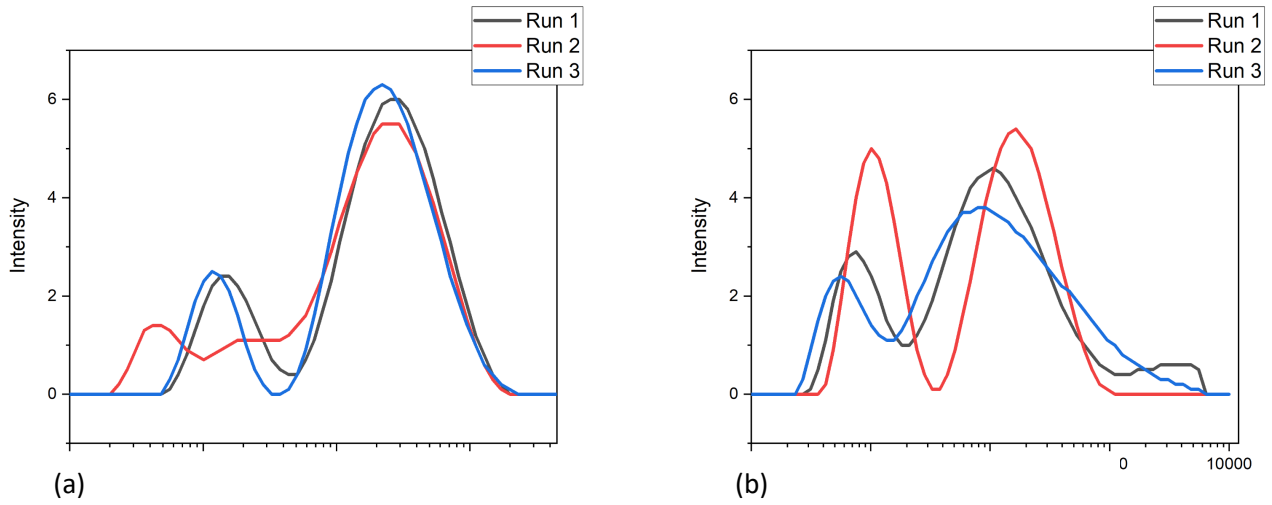

Figure 13: Particle size distribution of L-asparaginase NPs at a protein concentration of (a) 0.133 mg/ml, (b) 0.266 mg/ml

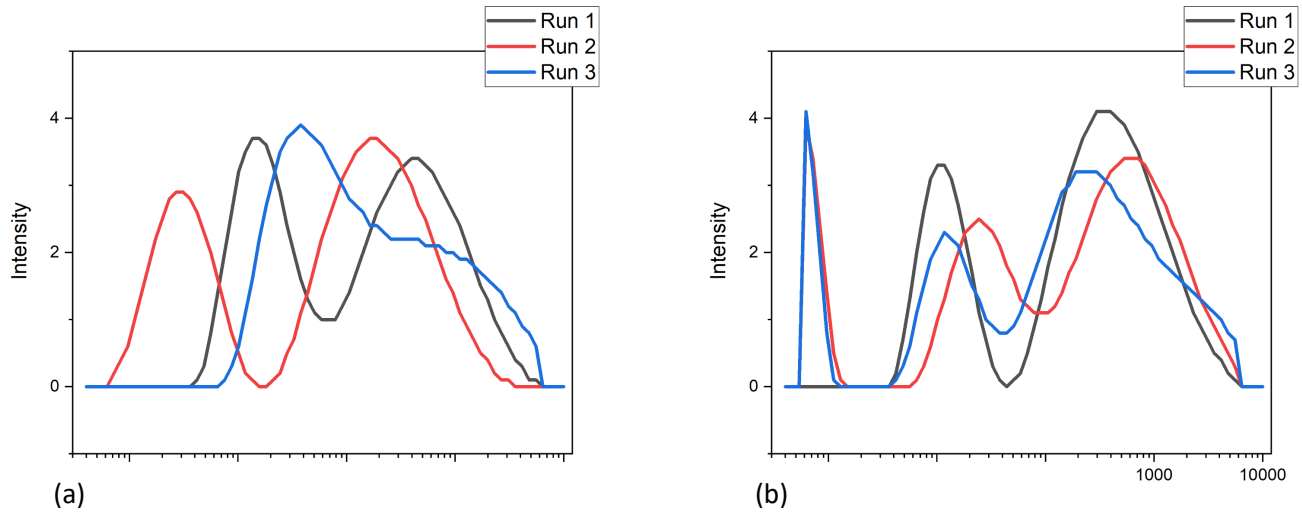

Figure 14: Particle size distribution of L-asparaginase NPs at a protein concentration of 0.266 mg/ml, (a) unfiltered (b) filtered

However, after careful consideration of the protein and polymer mixing technique in the particle synthesis procedure, later batches of NPs resulted in less polydispersity and an average

hydrodynamic diameter of 114.5 ± 5.66 nm. Figures 15 (a)-(j), show DLS data of L-asparaginase NPs at an initial protein concentration of 0.266 mg/ml taken at different time intervals after their synthesis. As shown below, this data confirms that these NPs are stable in solution for up to 6 months without aggregation. Long-term DLS measurements are in progress to evaluate if these particles are aggregating over time.

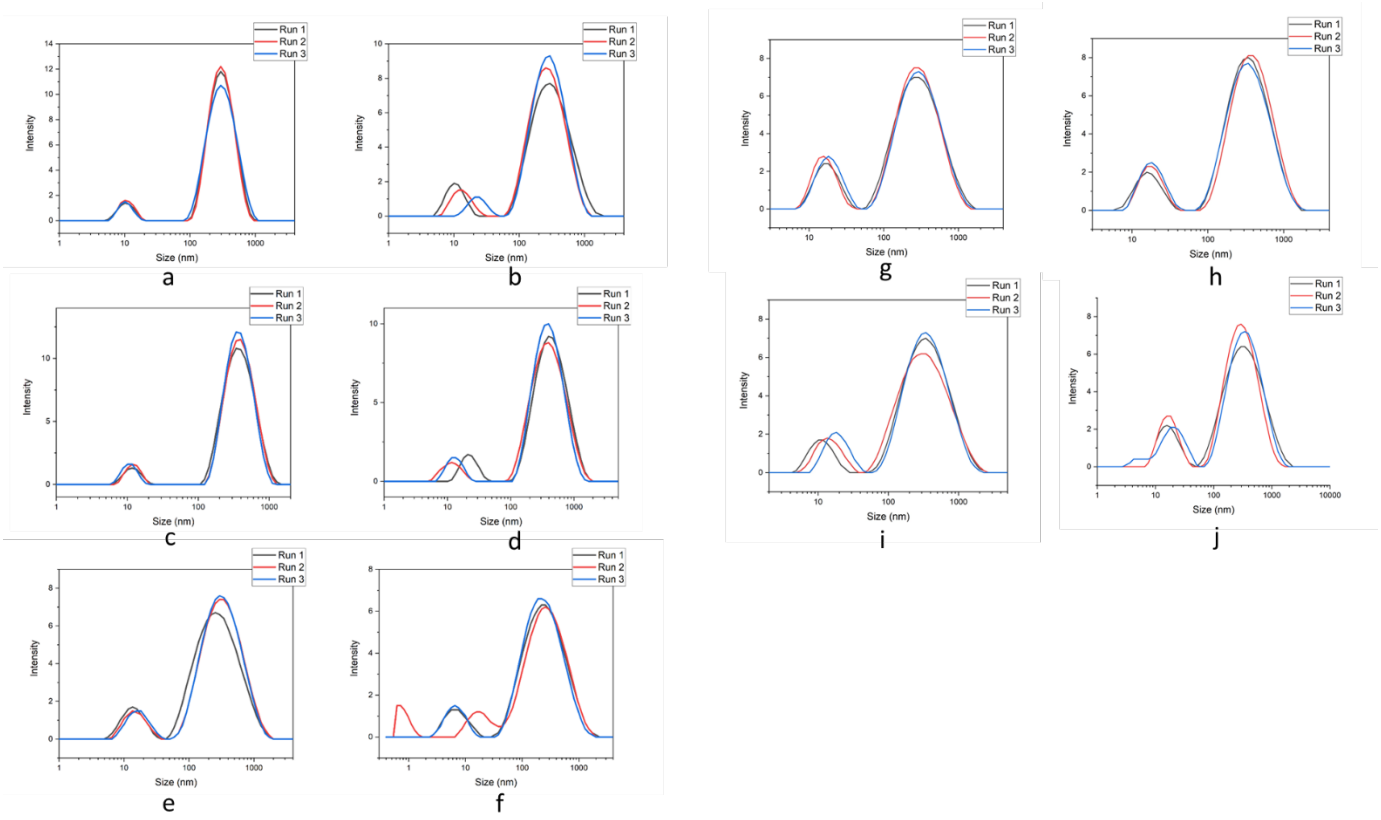

Figure 15: Particle size distribution of L-asparaginase NPs (0.266 mg/ml), (a) Freshly made NPs, (b) 3-days old NPs, (c) 8-days old NPs, (d) 10-days old NPs, (e) 15-days old NPs, (f) 17-days old NPs, (g) 46-days old NPs, (h) 53-days old NPs, (i) 56-days old, and (j) 6-months old

Table 4: Average hydrodynamic diameter of NP samples a-j

Sample	Average Hydrodynamic Diameter (nm)	PDI
a	196.77 ± 8.39	0.534
b	154.10 ± 12.00	0.604
c	255.67 ± 13.61	0.462
d	234.67 ± 12.39	0.591
e	153.17 ± 17.70	0.647
f	119.43 ± 7.94	0.677
g	85.34 ± 8.41	0.956
h	128.07 ± 20.24	0.845
i	136.07 ± 11.15	0.846
j	98.55 ± 16.74	0.986

The zeta potential of L-ASNase NPs was found to be 0.436 ± 0.258 mV. Figures 16 and 17 show the comparison of L-ASNase NPs synthesized with a vortex speed of 7 (Figure 16) and with a speed of 3.5 (Figure 17). The L-ASNase NPs synthesized with the vortex speed at 7 were found to have an average size of 135.5 nm and a PDI of 0.826. The L-ASNase NPs synthesized with the vortex speed at 3.5 were found to have an average size of 189.5 nm and a PDI of 0.572. As evident from the DLS data, changing the vortexing speed did not significantly affect the particle size.

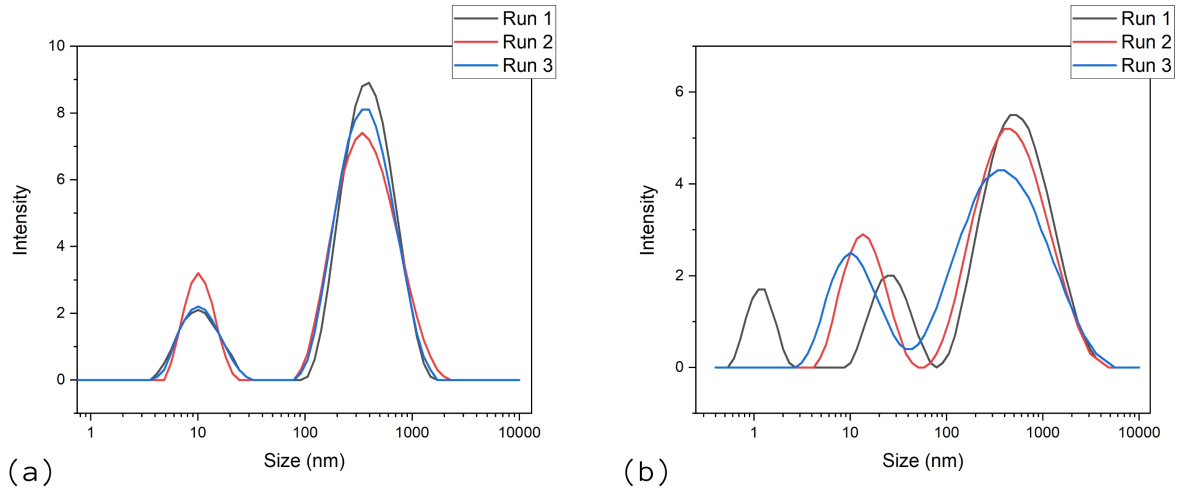

Figure 16: Particle size distribution of L-asparaginase NPs made at a vortex speed of 7 and at a protein concentration of 0.266 mg/ml, (a) Freshly made NPs, (b) 6-days old NPs,

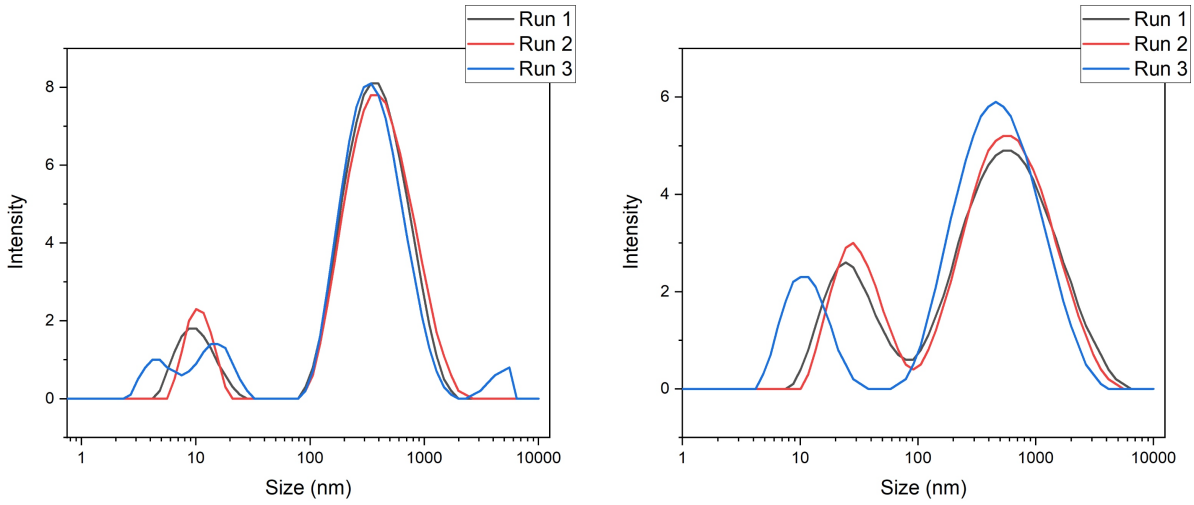

Figure 17: Particle size distribution of L-asparaginase NPs made at a vortex speed of 3.5 and at a protein concentration of 0.266 mg/ml, (a) Freshly made NPs, (b) 6-days old NPs,

3.3—Evaluation of L-ASNase Encapsulation Efficiency in NPs by SDS-PAGE

The extent of L-ASNase encapsulation was determined by a gel retardation assay. The results of 8% SDS-PAGE gel retardation assay are shown in Figure 18. Lane 2 shows the protein

ladder with molecular weight bands including 250, 130, 100, 70, 55, and 35 kDa. However, the protein ladder was not able to fully resolve in the 8% gel. The free L-ASNase control (lane 4) was able to freely migrate down the gel. PLL-g-PEG copolymer (lane 5) alone was not able to migrate down the gel. When PLL-g-PEG copolymer was added to L-ASNase, the protein was partially encapsulated and partial migration of L-ASNase down the gel was observed as shown in lane 6. Lane 7 shows filtered L-ASNase NPs.

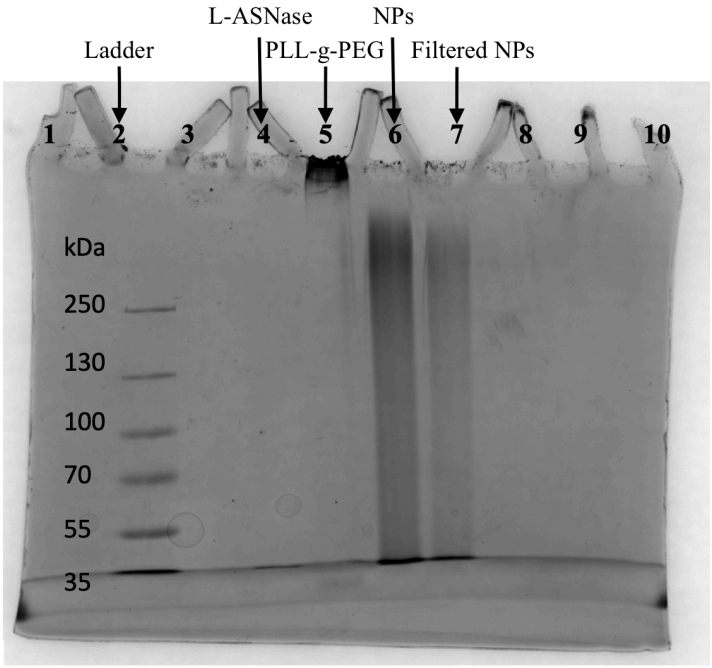

Figure 18: SDS-PAGE (8%) image of L-ASNase NPs

To extract more information from the gel and to achieve full resolution of the protein ladder, a 12% SDS-PAGE was used in future studies. Figure 19 shows 12% SDS-PAGE gel retardation assay results. As evident, 12% gel was able to fully resolve the protein ladder which is shown in Lane 2 with molecular weight bands including 250, 130, 100, 70, 55, 35, 25, 15 and 10 kDa. The free L-ASNase control (lane 4) was able to freely migrate down the gel. PLL-g-PEG copolymer (lane 5) alone was not able to migrate down the gel. When PLL-g-PEG copolymer was added to L-ASNase, the protein was fully encapsulated as shown in lane 6. Lane

7 shows filtered L-ASNase NPs. Therefore, based on lane 6 of the gel image shown in Figure 19, a 100% encapsulation was achieved in comparison to the gel image shown in Figure 18. is due to the difference in particle synthesis procedures as described in Table 1. 100% encapsulation of the protein was achieved by using the standard procedure reported in Table 1.

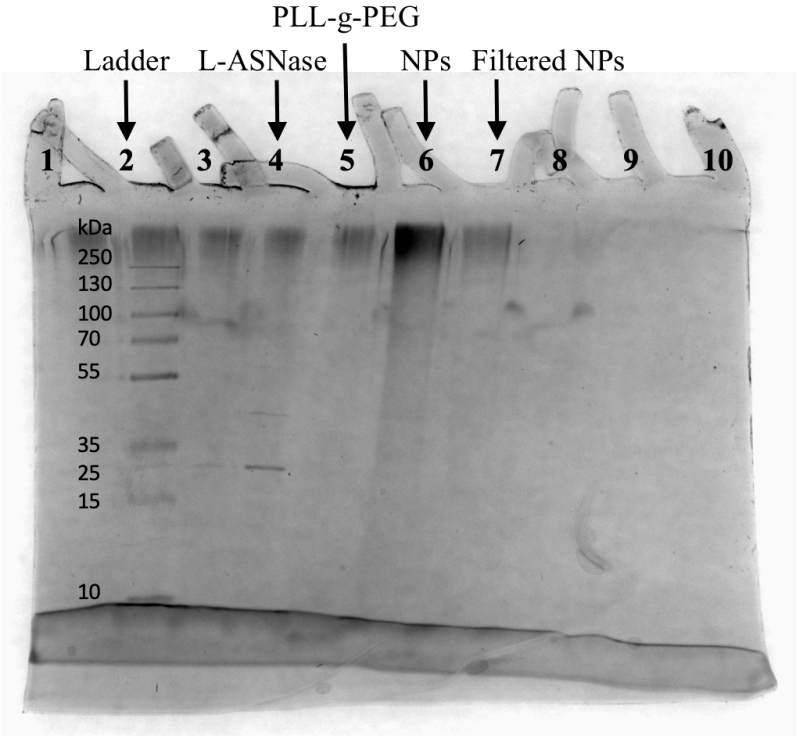

Figure 19: SDS-PAGE (12%) of L-ASNase NPs

Figure 20 shows 12% SDS-PAGE gels ran on 0-, 3-, 8-, 10-, 53-, and 56-, 3 months-, and 6 months-old NPs. Each gel shows similar band pattern to the gel shown in Figure 19. These results are evident that the NPs stay intact for more than 6 months in solution at physiological pH conditions. Long-term SDS-PAGE experiments are in progress.

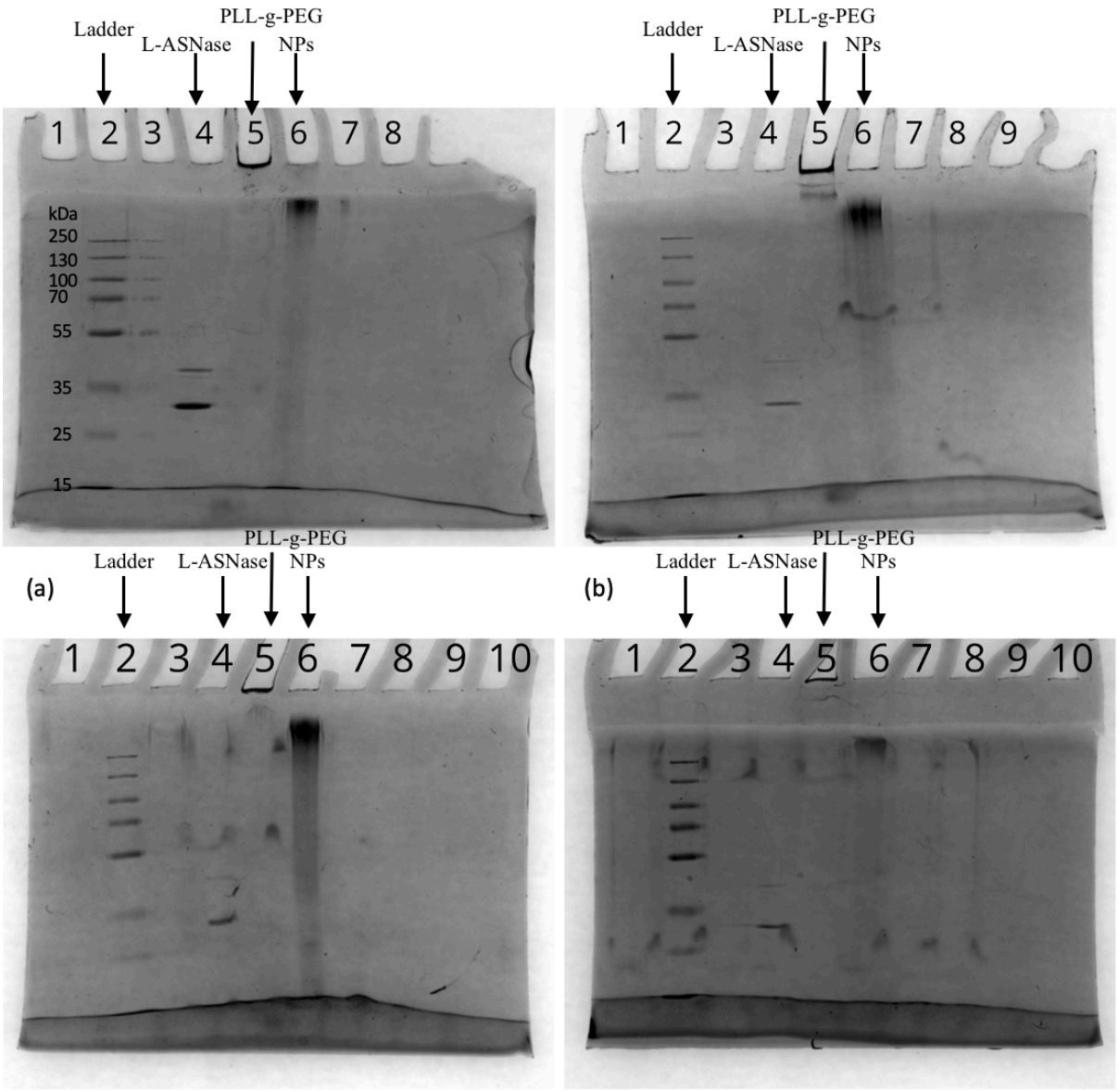
Ladder
L-ASNase
PLL-g-PEG
NPs
1 2 3 4 5 6 7 8
kDa
250
130
100
70
55
35
25
15
(a)
1 2 3 4 5 6 7 8 9
(b)
1 2 3 4 5 6 7 8 9 10
(c)
1 2 3 4 5 6 7 8 9 10
(d)

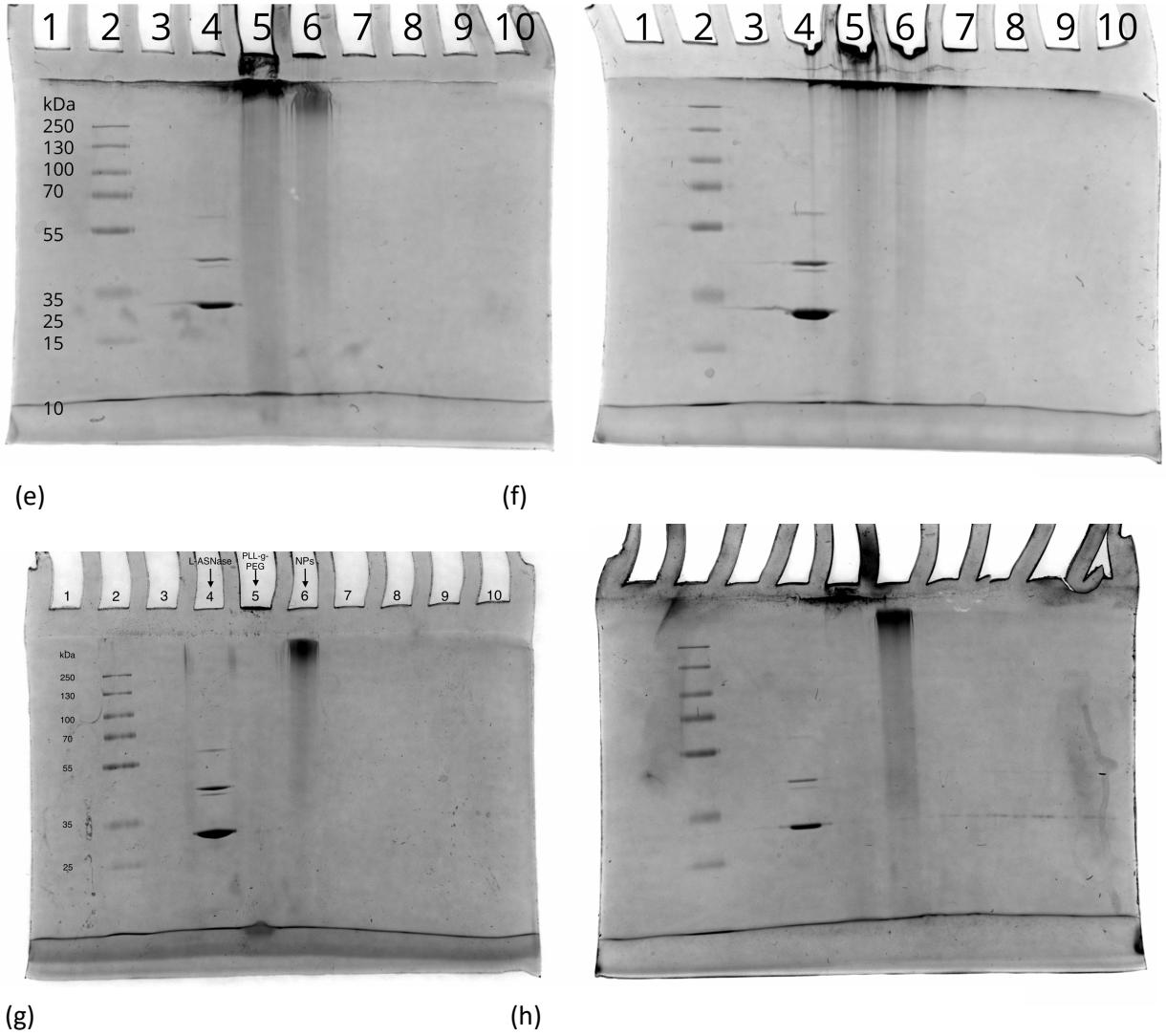

Figure 20: SDS-PAGE (12%) of L-ASNase NPs, (a) Fresh NPs, (b) 3-days old NPs, (c) 8-days old NPs, (d) 10-days old NPs**,** (e) 53-days old NPs, (f) 56-days old NPs**,** (g) 3 months old, and (h) 6 months old.

Native-PAGE gels were run to evaluate the size of the original protein that is encapsulated in nanoparticles. The results of the Native-PAGE gel are shown in Figure 21. The appearance of one protein gel band for L-ASNase (lane 4) confirmed that it starts as a tetramer. Although, L-ASNase has a size of 136.32 kDa, under our laboratory conditions, the L-ASNase native-PAGE gel band ran smaller than expected and appeared closer to 120 kDa.

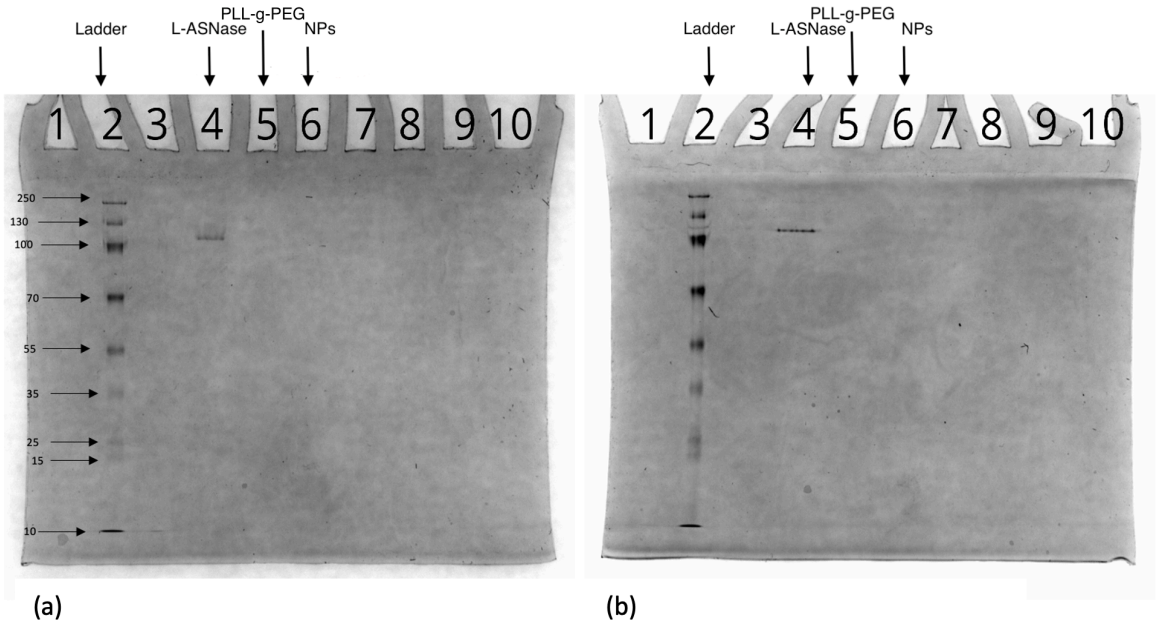

Figure 21: Native-PAGE (12%) of L-ASNase NPs, (a) 15-days and (b) 17-days old NPs

3.3.1— Evaluation of L-ASNase Encapsulation after Boiling Followed by SDS-PAGE

Free L-ASNase, PLL-g-PEG, and L-ASNase NPs were incubated at 95 °C for 5 minutes in a mixture of loading buffer, Laemmli SDS sample buffer (non-reducing), and 2-Mercaptoethanol. The purpose of this experiment was to prove the protein was encapsulated inside the NP construct and also to confirm the true size of the free enzyme, because boiling completely denatures the protein. The 2-Mercaptoethanol (BME) reduces disulfide bonds causing enzyme bands to be seen in lane 6. It is thought that the protein near the particle surface

got reduced by BME, causing some enzyme to escape encapsulation. In lane 6 of Figure 22, a band representing the encapsulated enzyme can be seen sitting in the stacker region. The free L-ASNase is represented by two bands between 35-55 kDa. The band near 35 kDa is believed to contain monomers of L-ASNase. The band closer to 45 kDa is speculated to be a monomer plus an additional unit of the enzyme. These bands match those seen in lane 4, containing boiled free L-ASNase. This experiment confirmed that our PLL-g-PEG NP construct contained encapsulated L-ASNase enzyme.

Figure 22: SDS-PAGE of boiled L-ASNase, PLL-g-PEG, and L-ASNase NPs

3.4—Measuring Asparaginase Activity in L-ASNase NPs

To evaluate how encapsulation could affect protein function, the asparaginase activity was determined by a coupled enzyme assay using a Sigma-Aldrich asparaginase activity assay

kit. The coupled enzyme assay works so that once L-ASNase has produced aspartate, an unknown enzyme reacts with aspartate to produce a colorimetric product. The colorimetric (570 nm) product is proportional to the aspartate generated and the asparaginase activity is reported as milliunit/mL, where one unit of asparaginase is defined as the amount of enzyme that catalyzes the formation of 1.0 mmole of aspartate per minute at 25 °C. Asparaginase activity in NPs was evaluated using a calibration curve for aspartate standards shown in Figure 23 and equation 1.

Equation 1: Asparaginase Activity

$$\text{Asparaginase Activity} = \frac{B \times \text{Sample Dilution Factor}}{(T_{final} - T_{initial}) \times V}$$

B is the amount of aspartate (nmole) generated between $T_{initial}$ and T_{final}, $T_{initial}$ is the time of first absorbance reading in minutes, T_{final} is the time of second reading in minutes, and V is the sample volume (mL) added to well. The L-ASNase activity in NPs calculated using equation 1 above showed an average (from 2 replicates) of 10.5 nmole/min/mL whereas the positive control (free L-ASNase) showed an average activity of 19.8 nmole/min/mL. Compared to the activity of the positive control reported above, NP showed 53% L-ASNase activity as a percentage. Encapsulation may affect the enzymatic activity of L-ASNase due to steric hindrance, diffusion-controlled access to the enzyme's active site, and conformational changes of the enzyme upon encapsulation. Therefore, the decrease in enzymatic activity observed in NPs could be due to one or more factors stated above.

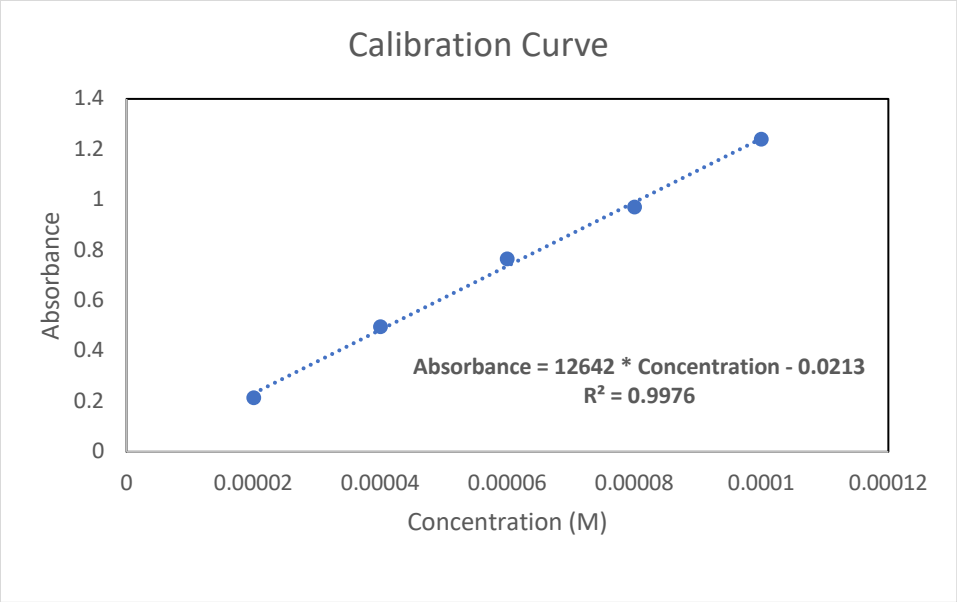

Figure 23: Calibration curve of the aspartate standards from the activity assay

3.5—Evaluation of NP Stability

Stability of NPs at physiological conditions was evaluated by measuring the possible release of encapsulated fluorescein isothiocynate (FITC)-BSA from the NPs incubated with 10% fetal bovine serum (FBS) at 37 °C as a function of time. Figure 24 shows an SDS-PAGE gel image for FITC-BSA NPs. This was done to confirm that we encapsulated the model enzyme, FITC-BSA, within the NP construct. The smearing may be due to the concentration of the sample or the addition of the fluorescent tag.

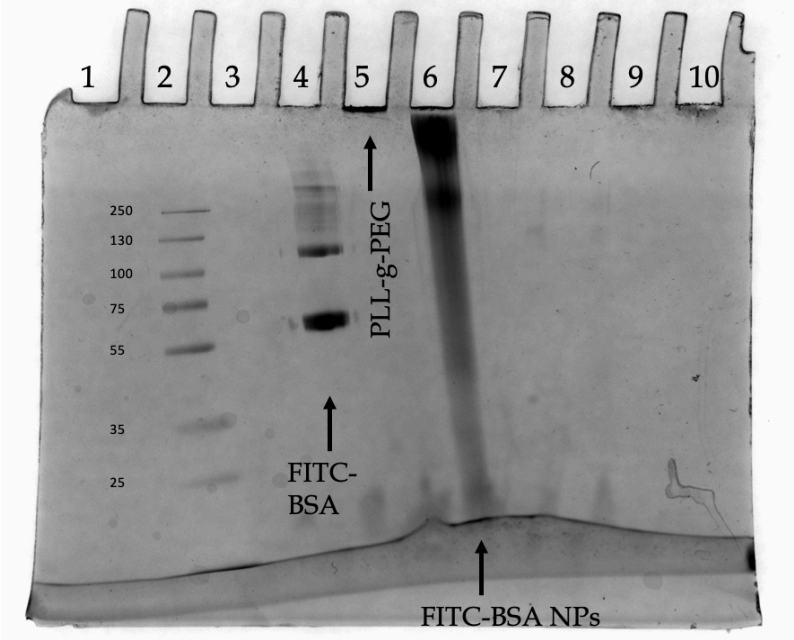

Figure 24: SDS-PAGE of FITC-BSA enzyme and FITC-BSA NPs

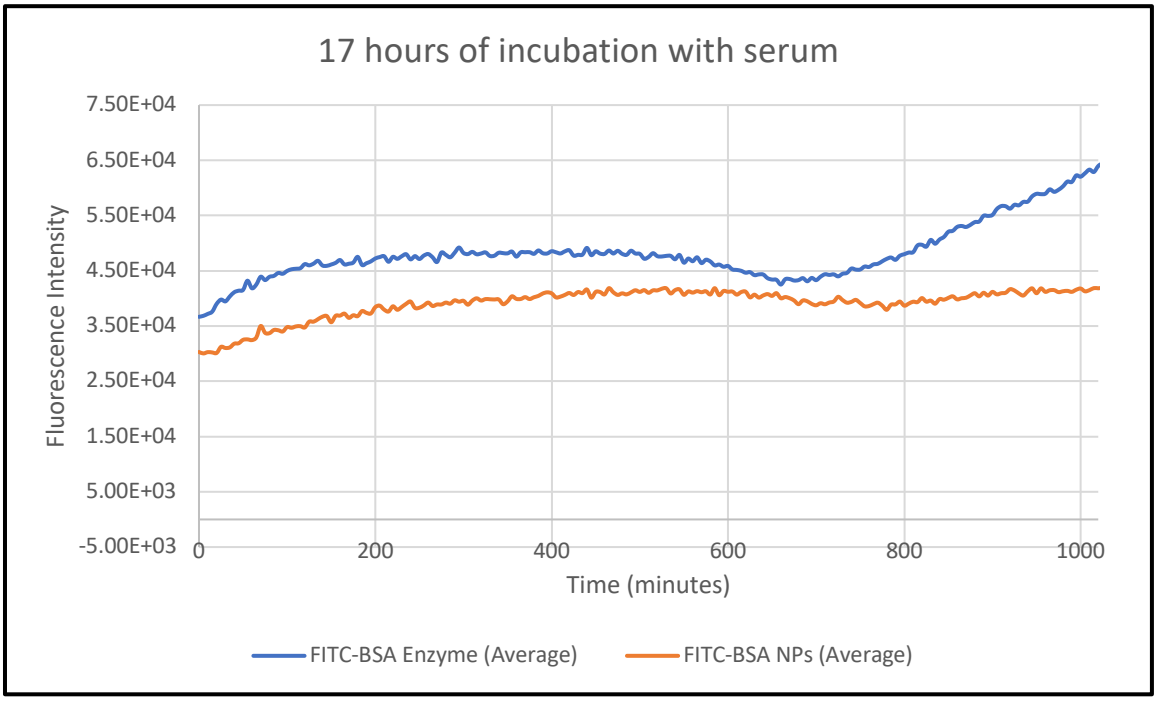

Figure 25: Fluorescence intensity of FITC-BSA enzyme and FITC BSA NPs over 17 hours.

The purpose of this experiment was to determine if the encapsulated enzymes escape the NP construct over time under physiological conditions. As shown in Figure 25, encapsulation of FITC-BSA in NPs resulted in a decrease in fluorescence intensity (~10,000 a.u.) due to self-quenching[21], compared to FITC-BSA alone. This is due to being encapsulated by PLL-g-PEG, when compared to free FITC-BSA. Over a period of 17 hrs., there was no distinctive changes observed in fluorescence intensity of NPs, indicating that there was no leaching of FITC-BSA from our NP constructs. Our results demonstrate that the NP constructs were able to effectively retain the encapsulated protein under physiological conditions at least up to 17 hours.

However, FITC-BSA itself found to self-quench. The enzyme is manufactured with an abundance of FITC tags to increase the sensitivity of detection. However, data from literature shows the opposite. The abundance of fluorophores resulted in a decrease of fluorescence. FITC molecules bound next to each other in a multiple-labeled protein can associate and form non fluorescent dimers. This is known as concentration quenching. Also, resonance energy transfer occurs from the excited state of a fluorescent FITC monomer to a non-fluorescent dimer. This results in an additional loss of fluorescence. Therefore, the increase in the fluorescence intensity of FITC-BSA after incubation at 37°C shown in Figure 25 can be explained by fluorescence dequenching. Since FITC-BSA is a highly quenched protein, the hydrolysis of only a few molecules will result in a noticeable increase in fluorescence intensity.[22] Free FITC-BSA showed this phenomenon after about 700 minutes in both Figures 25 and 26.

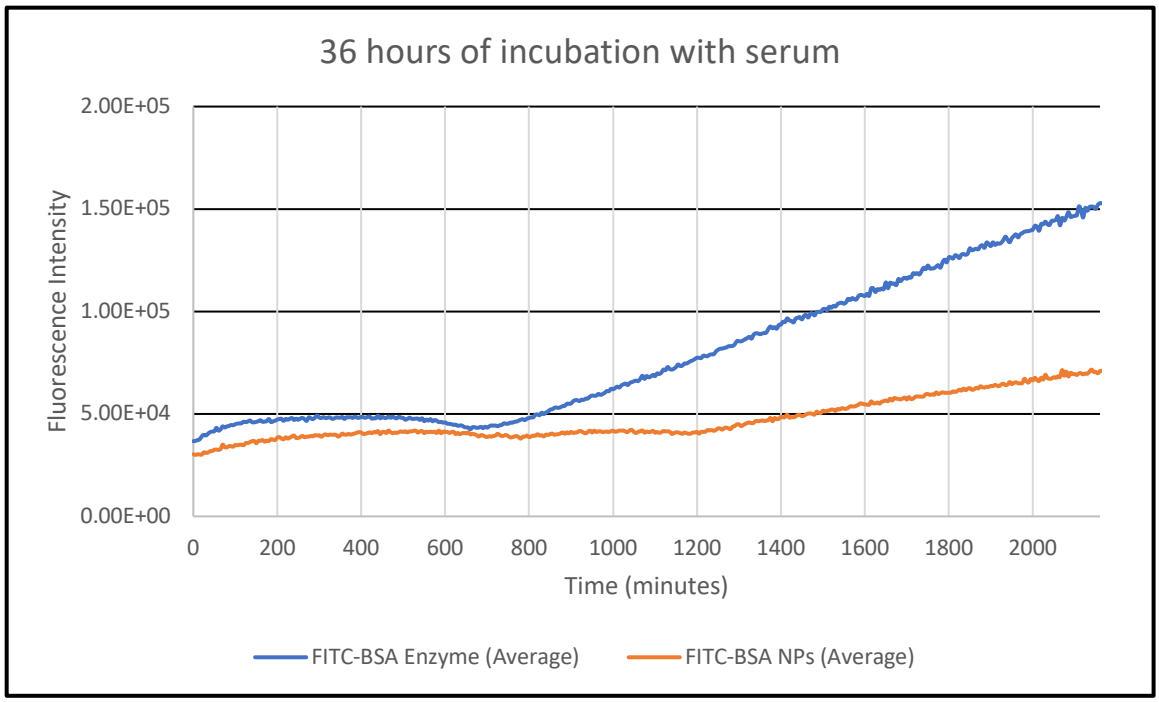

Figure 26: Fluorescence intensity of FITC-BSA enzyme and FITC BSA NPs over 36 hours.

The increase in fluorescence intensity for the FITC BSA NPs starting around 1200 minutes could be due to possible release of encapsulated FITC-BSA from NPs.

CHAPTER FOUR: CONCLUSIONS AND FUTURE DIRECTIONS

4.1—Conclusions

In the present study, we have successfully synthesized and characterized a maleimide functionalized PLL-g-PEG co-polymer. Nanoparticles were formed through electrostatic interactions of the cationic backbone of the PLL-g-PEG copolymer and negatively charged L-ASNase. L-ASNase nanoparticles had an average hydrodynamic diameter of 114.5 ± 5.66 nm and a near neutral zeta potential of 0.436 ± 0.258 mV. The extent of L-ASNase encapsulation was determined to be 100% according to the SDS-PAGE data. Additionally, SDS-PAGE data provides conclusive results that these therapeutic nanoparticles are stable in solution at physiological pH conditions for more than 6 months and long-term particle stability studies are in progress. Encapsulated L-ASNase showed an average of 10.5 nmole/min/mL activity and that is 53% as a percentage compared to the free L-ASNase positive control. These particles were stable in 10% FBS for more than 17 hours at 37 °C. In conclusion, we were able to successfully encapsulate a catalytically active, stable, therapeutic protein in PLL-g-PEG NPs.

4.2—Future Directions

Future studies of this project will focus on three broad areas including (1) in vivo delivery and targeting towards RBCs, (2) optimizing co-polymer architecture to increase the catalytic activity of encapsulated proteins, and (3) protein charge modelling to understand more about overall surface charge of these NPs. Functionalization of NP surface with RBC targeting peptides and cell penetrating peptides will be carried out to target these NPs towards RBCs *in vitro*. Studies evaluating the compatibility of these NPs with RBCs *in vitro* will also be carried out. *In vitro* uptake studies of functionalized NPs by RBCs will be evaluated using confocal

microscopy and flow cytometry. Further, we will evaluate the diffusion-controlled access of small molecules to the encapsulated enzyme by varying the copolymer architecture (grafting ratio) of the NPs. Encapsulation of proteins could affect their conformation. Therefore, possible conformational changes in the enzyme upon encapsulation will be studied using high resolution NMR spectroscopy. Further, surface charge of these NPs play a major role in their *in vivo* applications. We will extend our study in the area of protein charge modelling to understand more about the differences in surface charges seen in NPs encapsulating different types of proteins.

REFERENCES

(1) Jeevanandam, J.; Barhoum, A.; Chan, Y. S.; Dufresne, A.; Danquah, M. K. Review on Nanoparticles and Nanostructured Materials: History, Sources, Toxicity and Regulations. *Beilstein J. Nanotechnol.* **2018**, *9*, 1050–1074. https://doi.org/10.3762/bjnano.9.98.

(2) Li, J.; Cai, C.; Li, J.; Li, J.; Li, J.; Sun, T.; Wang, L.; Wu, H.; Yu, G. Chitosan-Based Nanomaterials for Drug Delivery. *Molecules* **2018**, *23* (10), 2661. https://doi.org/10.3390/molecules23102661.

(3) Patra, J. K.; Das, G.; Fraceto, L. F.; Campos, E. V. R.; Rodriguez-Torres, M. D. P.; Acosta-Torres, L. S.; Diaz-Torres, L. A.; Grillo, R.; Swamy, M. K.; Sharma, S.; Habtemariam, S.; Shin, H.-S. Nano Based Drug Delivery Systems: Recent Developments and Future Prospects. *J. Nanobiotechnology* **2018**, *16* (1), 71. https://doi.org/10.1186/s12951-018-0392-8.

(4) Kintzing, J. R.; Filsinger Interrante, M. V.; Cochran, J. R. Emerging Strategies for Developing Next-Generation Protein Therapeutics for Cancer Treatment. *Trends Pharmacol. Sci.* **2016**, *37* (12), 993–1008. https://doi.org/10.1016/j.tips.2016.10.005.

(5) Akash, M. S. H.; Rehman, K.; Tariq, M.; Chen, S. Development of Therapeutic Proteins: Advances and Challenges. *Turk. J. Biol.* **2015**, *39*, 343–358. https://doi.org/10.3906/biy-1411-8.

(6) Kaur, R.; Bhupinder, S. S. Enzymes as Drugs: An Overview. *Journal of Pharmaceutical Education and Research* **2012**, *3* (2), 29–41.

(7) Naff, N. J.; Carhuapoma, J. R.; Williams, M. A.; Bhardwaj, A.; Ulatowski, J. A.; Bederson, J.; Bullock, R.; Schmutzhard, E.; Pfausler, B.; Keyl, P. M.; Tuhrim, S.; Hanley, D. F. Treatment of Intraventricular Hemorrhage with Urokinase: Effects on 30-Day Survival. *Stroke* **2000**, *31* (4), 841–847. https://doi.org/10.1161/01.str.31.4.841.

(8) Liu, X.; Jin, L.-L.; Zhao, L.-L.; Wang, Y.-C.; Zhang, L.; Huang, Z.-Z.; Jin, H.-Q.; Liu, J.-Y.; Liang, Z.-J.; Liu, X.; Tan, H.; Ren, L.-J. In-Vivo Thrombolytic Efficacy of RGD Modified Protein-Polymer Conjugated Urokinase Nanogels. *Polym. Test.* **2021**, *104* (107392), 107392. https://doi.org/10.1016/j.polymertesting.2021.107392.

(9) Poly- L -lysine 0.1 (w/v) H2O 25988-63-0 https://www.sigmaaldrich.com/US/en/product/sigma/p8920 (accessed 2022 -03 -25).

(10) Verhoef, J. J. F.; Anchordoquy, T. J. Questioning the Use of PEGylation for Drug Delivery. *Drug Deliv. Transl. Res.* **2013**, *3* (6), 499–503. https://doi.org/10.1007/s13346-013-0176-5.

(11) Lubkowski J, Dauter M, Aghaiypour K, Wlodawer A, Dauter Z. Atomic resolution structure of *Erwinia chrysanthemi* L-asparaginase. Acta Crystallogr D Biol Crystallogr. 2003 Jan;59(Pt 1):84-92. doi: 10.1107/s0907444902019443. Epub 2002 Dec 19. PMID: 12499544.

DOI Citation:

Lubkowski, J., Dauter, Z. (2003) Atomic resolution structure of *Erwinia chrysanthemi* L-asparaginase doi: 10.2210/pdb1O7J/pdb

(12) Ulu, A.; Ates, B. Immobilization of L-Asparaginase on Carrier Materials: A Comprehensive Review. *Bioconjug. Chem.* **2017**, *28* (6), 1598–1610. https://doi.org/10.1021/acs.bioconjchem.7b00217.

(13) Bahreini, E.; Aghaiypour, K.; Abbasalipourkabir, R.; Mokarram, A. R.; Goodarzi, M. T.; Saidijam, M. Preparation and Nanoencapsulation of L-Asparaginase II in Chitosan-Tripolyphosphate Nanoparticles and in Vitro Release Study. *Nanoscale Res. Lett.* **2014**, *9* (1), 340. https://doi.org/10.1186/1556-276X-9-340.

(14) Wan, S.; He, D.; Yuan, Y.; Yan, Z.; Zhang, X.; Zhang, J. Chitosan-Modified Lipid Nanovesicles for Efficient Systemic Delivery of l-Asparaginase. *Colloids Surf. B Biointerfaces* **2016**, *143*, 278–284. https://doi.org/10.1016/j.colsurfb.2016.03.046.

(15) Avramis, V. I.; Tiwari, P. N. Asparaginase (Native ASNase or Pegylated ASNase) in the Treatment of Acute Lymphoblastic Leukemia. *Int. J. Nanomedicine* **2006**, *1* (3), 241–254.

(16) Gaydess, A.; Duysen, E.; Li, Y.; Gilman, V.; Kabanov, A.; Lockridge, O.; Bronich, T. Visualization of Exogenous Delivery of Nanoformulated Butyrylcholinesterase to the Central Nervous System. *Chem. Biol. Interact.* **2010**, *187* (1–3), 295–298. https://doi.org/10.1016/j.cbi.2010.01.005.

(17) Flynn, N.; Topal, Ç. Ö.; Hikkaduwa Koralege, R. S.; Hartson, S.; Ranjan, A.; Liu, J.; Pope, C.; Ramsey, J. D. Effect of Cationic Grafted Copolymer Structure on the Encapsulation of Bovine Serum Albumin. *Mater. Sci. Eng. C Mater. Biol. Appl.* **2016**, *62*, 524–531. https://doi.org/10.1016/j.msec.2016.01.092.

(18) Sahoo, K.; Koralege, R. S. H.; Flynn, N.; Koteeswaran, S.; Clark, P.; Hartson, S.; Liu, J.; Ramsey, J. D.; Pope, C.; Ranjan, A. Nanoparticle Attachment to Erythrocyte via the Glycophorin A Targeted ERY1 Ligand Enhances Binding without Impacting Cellular Function. *Pharm. Res.* **2016**, *33* (5), 1191–1203. https://doi.org/10.1007/s11095-016-1864-x.

(19) Sourav Bhattacharjee, DLS and zeta potential – What they are and what they are not?, Journal of Controlled Release, Volume 235, 2016, Pages 337-351, ISSN 0168-3659, https://doi.org/10.1016/j.jconrel.2016.06.017. (https://www.sciencedirect.com/science/article/pii/S0168365916303832)

(20) Stetefeld, J.; McKenna, S. A.; Patel, T. R. Dynamic Light Scattering: A Practical Guide and Applications in Biomedical Sciences. *Biophys. Rev.* **2016**, *8* (4), 409–427. https://doi.org/10.1007/s12551-016-0218-6.

(21) Hikkaduwa Koralege, R.; Sahoo, K.; Karumuri, S.; Flynn, N. H.; Liu, J.; Ranjan, A.; Pope, C.; Ramsey, J. D. Erythrocytes internalize nanoparticles functionalized with low molecular weight protamine. *Journal of Nanoparticle Research*, **2021**, 28(96), 1-16 https://doi.org/10.1007/s11051-021-05202-8

(22) Wischke C, Borchert HH. Fluorescein isothiocyanate labelled bovine serum albumin (FITC-BSA) as a model protein drug: opportunities and drawbacks. *Pharmazie*. **2006** Sep;61(9):770-4. PMID: 17020153.